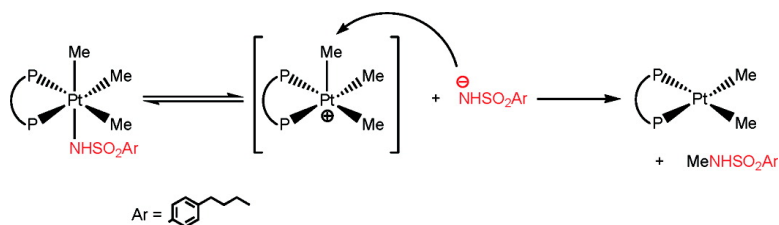


Alkyl Carbon–Nitrogen Reductive Elimination from Platinum(IV)–Sulfonamide Complexes

Andrew V. Pawlikowski, April D. Getty, and Karen I. Goldberg

J. Am. Chem. Soc., **2007**, 129 (34), 10382–10393 • DOI: 10.1021/ja069191h • Publication Date (Web): 02 August 2007

Downloaded from <http://pubs.acs.org> on February 15, 2009



More About This Article

Additional resources and features associated with this article are available within the HTML version:

- Supporting Information
- Links to the 9 articles that cite this article, as of the time of this article download
- Access to high resolution figures
- Links to articles and content related to this article
- Copyright permission to reproduce figures and/or text from this article

[View the Full Text HTML](#)

Alkyl Carbon–Nitrogen Reductive Elimination from Platinum(IV)–Sulfonamide Complexes

Andrew V. Pawlikowski, April D. Getty, and Karen I. Goldberg*

Contribution from the Department of Chemistry, University of Washington, P.O. Box 351700, Seattle, Washington 98195-1700

Received December 21, 2006; E-mail: goldberg@chem.washington.edu

Abstract: Platinum(IV) complexes containing monodentate sulfonamide ligands, *fac*-(dppbz)PtMe₃(NHSO₂R) (dppbz = *o*-bis(diphenylphosphino)benzene; R = *p*-C₆H₄(CH₂)₃CH₃ (**1a**), *p*-C₆H₄CH₃ (**1b**), CH₃ (**1c**)), have been synthesized and characterized, and their thermal reactivity has been explored. Compounds **1a–c** undergo competitive C–N and C–C reductive elimination upon thermolysis to form *N*-methylsulfonamides and ethane, respectively. Selectivity for either C–N or C–C bond formation can be achieved by altering the reaction conditions. Good yields of the C–N-coupled products were observed when the thermolyses of **1a–c** were conducted in benzene-*d*₆. In contrast, exclusive C–C reductive elimination occurred upon thermolysis of **1a,b** in nitrobenzene-*d*₅. When the thermolyses of **1a** were performed in the presence of sulfonamide anion NHSO₂R[−] in benzene-*d*₆, ethane elimination was completely inhibited and C–N reductive elimination products were formed in high yield. Mechanistic studies support a two-step reaction pathway involving initial dissociation of NHSO₂R[−] from the platinum center, followed by nucleophilic attack of this anion on a methyl group of the resulting five-coordinate platinum(IV) cation to form MeNHSO₂R and (dppbz)-PtMe₂. C–C reductive elimination to form ethane occurs directly from the five-coordinate Pt(IV) cation.

Introduction

Amines and their derivatives are widely used in the chemical industry as dyes, surfactants, pharmaceutical agents, and specialty chemicals. As a result, the development of new, facile synthetic procedures for the formation of carbon–nitrogen bonds is the subject of much current research.¹ One prominent example that has emerged over the past decade is the synthesis of aromatic amines from aryl halides and primary or secondary amines catalyzed by Pd(II) or Ni(II) complexes, developed by the groups of Hartwig² and Buchwald.³ Detailed mechanistic studies of these C–N bond-forming reactions support aryl C–N reductive elimination from the M(II) center as the critical product release step of the catalytic cycle.^{2,3} A number of other C–N reductive elimination reactions have been reported in recent years from low-valent, late transition metal centers such as Pd(II)⁴ or Ru(II),⁵ all involving sp²-hybridized carbon atoms. Examples of C(sp³)–N reductive elimination, a potentially important reaction step in the formation of alkyl amines, are

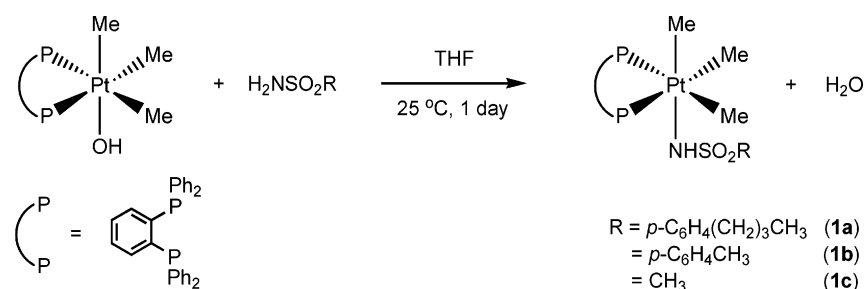
extremely scarce.^{6,7} Hillhouse has reported oxidatively induced C(sp³)–N reductive eliminations from Ni(II) complexes that proceed upon a one-electron oxidation to Ni(III). Such reactions with Ni(II) metallacycles produced cyclic amines in high yields,^{6,7} but reactions of acyclic complexes produced tertiary amines in low yields.⁶ Closely related to C(sp³)–N reductive elimination reactions, intramolecular nucleophilic attack of an amino group on axial alkyl groups attached to Rh(III) porphyrin complexes to form pyrrolidines has recently been documented.⁸

Since many catalytic systems involve oxidative addition of substrate to a d⁸ metal complex followed by reductive elimination from a d⁶ center later in the cycle,⁹ the examination of C–N bond forming reductive elimination from high-valent d⁶ metal complexes could play a crucial role in the rational development of novel catalysts and catalytic amination reactions.

- (1) (a) Brunet, J. J.; Neibacker, D.; Niedercorn, F. *J. Mol. Catal.* **1989**, *49*, 235. (b) Lawrence, S. A. *Amines: Synthesis, Properties and Applications*; Cambridge University Press: New York, 2004. (2) (a) Hartwig, J. F. *Angew. Chem., Int. Ed.* **1998**, *37*, 2046. (b) Hartwig, J. F. *Acc. Chem. Res.* **1998**, *31*, 852. (c) Hartwig, J. F. *Pure Appl. Chem.* **1999**, *71*, 1417. (d) Hartwig, J. F. In *Handbook of Organopalladium Chemistry for Organic Synthesis*; Negishi, E. I., Ed.; Wiley-Interscience: New York, 2002; Vol. 1, p 1051. (e) Hartwig, J. F. *Synlett* **2006**, 1283. (f) Shekhar, S.; Ryberg, P.; Hartwig, J. F.; Mathew, J. S.; Blackmond, D. G.; Strieter, E. R.; Buchwald, S. L. *J. Am. Chem. Soc.* **2006**, *128*, 3584. (g) Hartwig, J. F. *Inorg. Chem.* **2007**, *46*, 1936. (3) (a) Wolfe, J. P.; Wagaw, S.; Marcoux, J.-F.; Buchwald, S. L. *Acc. Chem. Res.* **1998**, *31*, 805. (b) Yang, B. H.; Buchwald, S. L. *J. Organomet. Chem.* **1999**, *576*, 125. (c) Muci, A. R.; Buchwald, S. L. *Top. Curr. Chem.* **2002**, *219*, 131. (d) See ref 2f.

- (4) (a) Paul, F.; Patt, J.; Hartwig, J. F. *J. Am. Chem. Soc.* **1994**, *116*, 5969. (b) Driver, M. S.; Hartwig, J. F. *J. Am. Chem. Soc.* **1995**, *117*, 4708. (c) Guram, A. S.; Rennels, Buchwald, S. L. *Angew. Chem., Int. Ed.* **1995**, *34*, 1348. (d) Driver, M. S.; Hartwig, J. F. *J. Am. Chem. Soc.* **1997**, *119*, 8232. (e) Wagaw, S.; Rennels, R. A.; Buchwald, S. L. *J. Am. Chem. Soc.* **1997**, *119*, 8451. (f) Hartwig, J. F. *Angew. Chem., Int. Ed.* **1998**, *37*, 2090. (g) Mann, G.; Hartwig, J. F.; Driver, M. S.; Fernandez-Rivas, C. *J. Am. Chem. Soc.* **1998**, *120*, 827. (h) Carbayo, A.; Cuevas, J. V.; Garcia-Herbosa, G. *J. Organomet. Chem.* **2002**, *658*, 15. (i) Yamashita, M.; Cuevas Vicario, J. V.; Hartwig, J. F. *J. Am. Chem. Soc.* **2003**, *125*, 16347. (5) Abbenhuis, H. C. L.; Pfeffer, M.; Sutter, J.-P.; de Cian, A.; Fischer, J.; Ji, H. L.; Nelson, J. H. *Organometallics* **1993**, *12*, 4464. (6) Koo, K.; Hillhouse, G. L. *Organometallics* **1995**, *14*, 4421. (7) (a) Koo, K.; Hillhouse, G. L. *Organometallics* **1996**, *15*, 2669. (b) Lin, B. L.; Clough, C. R.; Hillhouse, G. L. *J. Am. Chem. Soc.* **2002**, *124*, 2890. (8) Sanford, M. S.; Groves, J. T. *Angew. Chem., Int. Ed.* **2004**, *43*, 588. (9) (a) Crabtree, R. H. *The Organometallic Chemistry of the Transition Metals*, 4th ed.; John Wiley & Sons: New York, 2005. (b) Parshall, G. W.; Ittel, S. D. *Homogeneous Catalysis: The Applications and Chemistry of Catalysis by Soluble Transition Metal Complexes*, 2nd ed.; Wiley-Interscience: New York, 1992.

Scheme 1



Notably, however, examples of C–N reductive elimination reactions from high-valent d^6 metals such as Pt(IV), Pd(IV), Ir(III), or Rh(III)⁸ are exceedingly rare.

Our group has previously reported $\text{C}(\text{sp}^3)\text{--O}$ and $\text{C}(\text{sp}^3)\text{--I}$ reductive elimination reactions from d^6 Pt(IV) complexes of the type $\text{fac-L}_2\text{PtMe}_3\text{X}$ ($\text{L}_2 = \text{bis}(\text{diphenylphosphino})\text{ethane}$ (dppe), *o*-bis(diphenylphosphino)benzene (dppbz); $\text{X} = \text{OAr}$, $\text{OC}(\text{O})\text{R}$, I).^{10,11} Herein we report related Pt(IV)-amido complexes and investigations of their thermal reactivity. The Pt(IV)–sulfonamide complexes $\text{fac-(dppbz)PtMe}_3(\text{NHSO}_2\text{R})$ ($\text{R} = p\text{-C}_6\text{H}_4(\text{CH}_2)_3\text{CH}_3$ (**1a**), $p\text{-C}_6\text{H}_4\text{CH}_3$ (**1b**), CH_3 (**1c**)) have been synthesized and characterized. Alkyl C–N reductive elimination from **1a–c** is observed upon thermolysis, and *N*-methylsulfonamides are formed in good yields. The reactions reported here are not only rare examples of alkyl C–N coupling reactions mediated by a metal center^{6–8} but also represent the first examples of directly observed alkyl C–N reductive elimination from a high-valent, late transition metal center. The C–N coupling reactions to form alkylsulfonamide linkages may also be useful in organic synthesis, as the sulfonyl moiety can function as an amine-protecting group, with deprotection to yield primary or secondary amines.¹²

Results

Synthesis and Characterization of $\text{fac-(dppbz)PtMe}_3(\text{NHSO}_2\text{R})$ ($\text{R} = p\text{-C}_6\text{H}_4(\text{CH}_2)_3\text{CH}_3$, $p\text{-C}_6\text{H}_4\text{CH}_3$, CH_3) (1a–c**).** To date there are very few reported examples of Pt(IV) complexes containing monodentate amido ligands.¹³ Our initial attempts to prepare Pt(IV) complexes, $\text{fac-L}_2\text{PtMe}_3\text{X}$, where $\text{X} = \text{amido}$, were modeled after the successful preparation of similar aryloxide complexes ($\text{X} = \text{OAr}$).¹⁰ However, metathesis reactions of $\text{fac-(dppbz)PtMe}_3\text{X}$ ($\text{X} = \text{I}$, OAc , O_2CCF_3) with amide salts such as KNHPH, KNPh₂, KNHSO₂($p\text{-C}_6\text{H}_4\text{CH}_3$), or LiNC₅H₁₀ resulted in either immediate reduction of the platinum to produce (dppbz)PtMe₂ or the formation of the desired Pt(IV)–amido complex occurred at a comparable rate to the reduction of the platinum such that isolation of the Pt(IV)–amido species was not practical.

A more successful strategy was based on the reported syntheses of bridging Pd(II)– and Pt(II)–amido complexes via the reaction of the analogous bridging Pd(II)– and Pt(II)–

hydroxo dimers with amines.¹⁴ Thus, the reactions of the monomeric Pt(IV)–hydroxo complex $\text{fac-(dppbz)PtMe}_3(\text{OH})$ ¹⁵ with aniline and various sulfonamides were investigated. The reaction with aniline did not produce a significant amount of the desired Pt(IV)–anilido complex, and rapid reduction to Pt(II) was observed. Notably, however, the condensation reaction of $\text{fac-(dppbz)PtMe}_3(\text{OH})$ with an excess of sulfonamide, H₂NSO₂R, in THF at room temperature allowed isolation of the Pt(IV)–sulfonamide complexes $\text{fac-(dppbz)PtMe}_3(\text{NHSO}_2\text{R})$ ($\text{R} = p\text{-C}_6\text{H}_4(\text{CH}_2)_3\text{CH}_3$ (**1a**), $p\text{-C}_6\text{H}_4\text{CH}_3$ (**1b**), CH_3 (**1c**)) (Scheme 1). Compounds **1a–c** are unusual in that relatively few high oxidation state, late transition metal complexes containing monodentate amido ligands have been reported.^{13,16}

The Pt(IV)–sulfonamide complexes **1a–c** were isolated as white, air-stable solids in 60–65% yield and were characterized by ¹H and ³¹P NMR spectroscopy. Compound **1a** was also characterized by X-ray crystallography. The ORTEP diagram of **1a** is shown in Figure 1, and selected bond lengths and angles are presented in Table 1.¹⁷

The Pt–C and Pt–P bond lengths are comparable to related $\text{fac-L}_2\text{PtMe}_3\text{X}$ ($\text{L}_2 = \text{dppe}$, dppbz; $\text{X} = \text{I}$, OAr , $\text{OC}(\text{O})\text{R}$) complexes (Pt–C_{trans to P} = 2.09–2.10 Å, Pt–C_{trans to X} = 2.06–2.08 Å, Pt–P = 2.35–2.38 Å).^{10,11} The Pt–N bond length of 2.199(4) Å is the longest reported Pt(IV)–N bond length for structurally characterized monomeric Pt(IV)–amide complexes (Pt–N = 2.06–2.15 Å),^{13,18} presumably as a result of the strong trans effect of the apical methyl ligand coupled with the poor donating ability of the sulfonamide ligand.¹⁹

The ¹H and ³¹P{¹H} NMR data for **1a–c** confirm that a similar structure with a facial arrangement of the three methyl

- (10) (a) Williams, B. S.; Holland, A. W.; Goldberg, K. I. *J. Am. Chem. Soc.* **1999**, *121*, 252. (b) Williams, B. S.; Goldberg, K. I. *J. Am. Chem. Soc.* **2001**, *123*, 2576.
- (11) (a) Goldberg, K. I.; Yan, J.; Winter, E. L. *J. Am. Chem. Soc.* **1994**, *116*, 1573. (b) Goldberg, K. I.; Yan, J.; Breitung, E. M. *J. Am. Chem. Soc.* **1995**, *117*, 6889.
- (12) Greene, T. W.; Wuts, P. G. M. *Protective Groups in Organic Synthesis*, 3rd ed.; John Wiley & Sons: New York, 1999; p 603.
- (13) (a) Müller, G.; Riede, J.; Beyerle-Pfnur, R.; Lippert, B. *J. Am. Chem. Soc.* **1984**, *106*, 7999. (b) Renn, O.; Lippert, B.; Albinati, A.; Lianza, F. *Inorg. Chim. Acta* **1993**, *211*, 177.

- (14) (a) Ruiz, J.; Martínez, M. T.; Vicente, C.; García, G.; López, G.; Chaloner, P. A.; Hitchcock, P. B. *Organometallics* **1993**, *12*, 4321. (b) Driver, M. S.; Hartwig, J. F. *J. Am. Chem. Soc.* **1996**, *118*, 4206. (c) Driver, M. S.; Hartwig, J. F. *Organometallics* **1997**, *16*, 5706. (d) Ruiz, J.; Rodríguez, V.; López, G.; Casabo, J.; Molins, E.; Miravittles, C. *Organometallics* **1999**, *18*, 1177. (e) Li, J. J.; Li, W.; James, A.; Holbert, T.; Sharp, T.; Sharp, P. R. *Inorg. Chem.* **1999**, *38*, 1563. (f) Getty, A. D.; Goldberg, K. I. *Organometallics* **2001**, *20*, 2545.
- (15) Smythe, N. A. *Reactivity Studies of Platinum(IV) Hydroxide and Methoxide Complexes and the Study of Pincer Palladium(II) Complexes as Potential Catalysts for Olefin Epoxidation*. Ph.D. Thesis, University of Washington, Seattle, WA, 2004.
- (16) (a) Bryndza, H. E.; Tam, W. *Chem. Rev.* **1988**, *88*, 1163. (b) Fryzuk, M. D.; Montgomery, C. D. *Coord. Chem. Rev.* **1989**, *95*, 1. (c) Glueck, D. S.; Winslow, L. J. N.; Bergman, R. G. *Organometallics* **1991**, *10*, 1462. (d) Kaplan, A. W.; Ritter, J. C. M.; Bergman, R. G. *J. Am. Chem. Soc.* **1998**, *120*, 6828. (e) Fulton, J. R.; Holland, A. W.; Fox, D. J.; Bergman, R. G. *Acc. Chem. Res.* **2002**, *35*, 44. (f) Kanzelberger, M.; Zhang, X.; Emge, T. J.; Goldman, A. S.; Zhao, J.; Incarvito, C.; Hartwig, J. F. *J. Am. Chem. Soc.* **2003**, *125*, 13644. (g) Rais, D.; Bergman, R. G. *Chem.–Eur. J.* **2004**, *10*, 3970. (h) Zhao, J.; Goldman, A. S.; Hartwig, J. F. *Science* **2005**, *307*, 1080.
- (17) Complete X-ray crystallographic data are provided in the Supporting Information.
- (18) (a) Campbell, C. J.; Castineiras, A.; Nolan, K. B. *J. Chem. Soc., Chem. Commun.* **1995**, 19, 1939. (b) Koz'min, P. A.; Surazhskyy, M. D.; Baranovskii, I. B. *Russ. J. Inorg. Chem.* **2001**, *9*, 1342.
- (19) Becker, J. J.; White, P. S.; Gagne, M. R. *Inorg. Chem.* **1999**, *38*, 798.

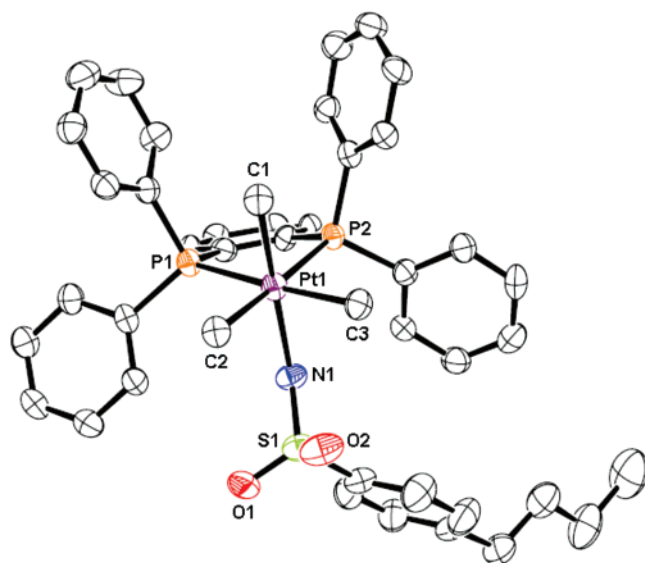


Figure 1. ORTEP diagram of *fac*-(dppbz)PtMe₃(NHSO₂(*p*-C₆H₄(CH₂)₃-CH₃)) (**1a**). Thermal ellipsoids are shown at the 50% probability level. Hydrogen atoms, disorder in the butyl chain, and molecules of THF and ether have been omitted for clarity.

Table 1. Selected Bond Lengths and Angles in the Crystal Structure of **1a**

bond lengths (Å)		bond angles (deg)	
Pt–C(1)	2.092(5)	C(1)–Pt–C(3)	88.6(2)
Pt–C(2)	2.108(5)	C(1)–Pt–C(2)	84.5(2)
Pt–C(3)	2.108(5)	C(3)–Pt–C(2)	88.5(2)
Pt–N(1)	2.199(4)	C(3)–Pt–N(1)	88.40(19)
Pt–P(1)	2.3569(13)	C(2)–Pt–N(1)	92.53(18)
Pt–P(2)	2.3659(13)	C(1)–Pt–P(2)	93.85(15)
N(1)–S(1)	1.583(4)	C(3)–Pt–P(2)	92.28(15)
S(1)–O(1)	1.439(4)	N(1)–Pt–P(2)	89.13(12)
S(1)–O(2)	1.439(4)	C(1)–Pt–P(1)	90.77(16)
		C(2)–Pt–P(1)	95.39(15)
		N(1)–Pt–P(1)	92.42(12)
		P(1)–Pt–P(2)	83.75(4)
		C(1)–Pt–N(1)	175.85(18)
		C(3)–Pt–P(1)	175.94(15)
		C(2)–Pt–P(2)	178.17(15)
		Pt–N(1)–S(1)	130.3(3)

ligands is maintained in solution. Only one resonance with Pt satellites is observed in the ³¹P NMR spectra of **1a–c**, indicating two equivalent phosphorus atoms. In the ¹H NMR spectra, the Pt-bound methyl groups give rise to a triplet and a virtual triplet with Pt satellites in a 1:2 ratio; the signal for the axial methyl group (0.32 ppm, 3H, ³J_{P–H} = 7.5 Hz, ²J_{Pt–H} = 67 Hz for **1a**) is shifted upfield from the equatorial methyl groups (1.89 ppm, 6H, ³J_{P–H} = 7.0 Hz, ²J_{Pt–H} = 60 Hz). The chemical shifts and coupling constants for the Pt-bound methyl groups are comparable with the values reported for other *fac*-L₂PtMe₃X complexes.^{10,11,15} The chemical shifts of the protons on the Pt-bound sulfonamide moiety are similar to the free sulfonamide H₂NSO₂R, with the exception that the N–H protons of **1a–c** are shifted upfield by almost 2 ppm. For example, the N–H proton of **1a** resonates at 1.77 ppm and the N–H protons of H₂NSO₂(*p*-C₆H₄(CH₂)₃CH₃) resonate at 3.57 ppm in C₆D₆.

Thermolysis of 1a. Products from both C–N reductive elimination ((dppbz)PtMe₂ (**2**) and MeNHSO₂(*p*-C₆H₄(CH₂)₃CH₃) (**3a**)) and C–C reductive elimination (ethane and (dppbz)-PtMe(NHSO₂(*p*-C₆H₄(CH₂)₃CH₃)) (**4a**)) were observed upon thermolysis of **1a** at 100 °C in C₆D₆ (Scheme 2). An additional

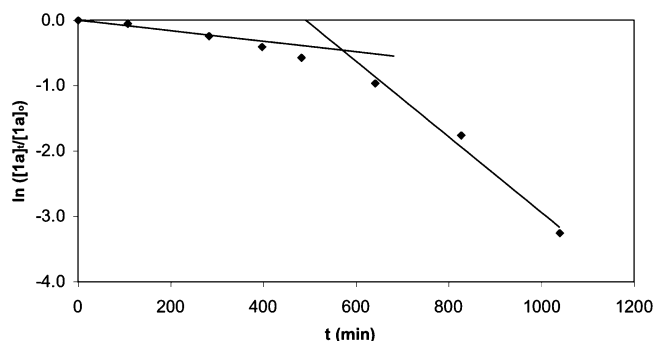


Figure 2. First-order kinetic plot of thermolysis of **1a** ([**1a**]₀ = 5 mM) in C₆D₆ at 100 °C.

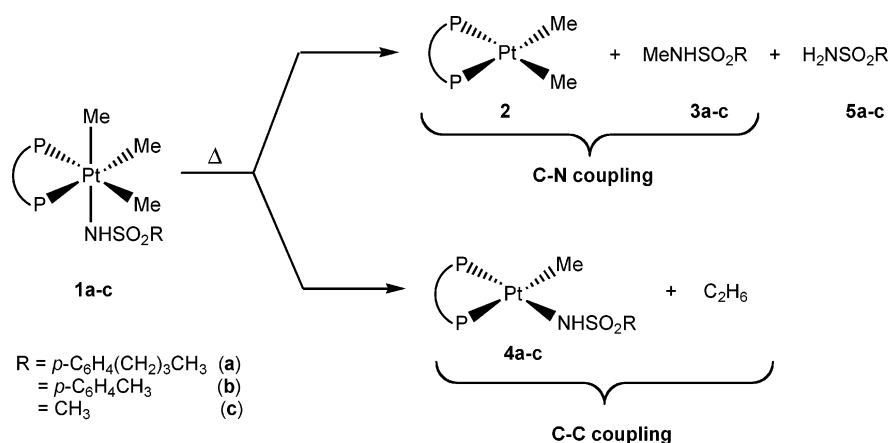
sulfonamide product, H₂NSO₂(*p*-C₆H₄(CH₂)₃CH₃) (**5a**) and a small amount of methanol (<5%) were also observed in the thermolysis reaction of **1a**. Integration of the ¹H NMR signal for the methyl groups of **2** relative to an internal standard indicated 69% conversion to **2**, the platinum product of C–N coupling. However, **3a**, the organic product of C–N coupling, was formed in only 48% yield. The additional sulfonamide product **5a** was produced in 18% yield. Thus, the sum of the yields of the organic sulfonamides **3a** and **5a** (66%) is equivalent to the amount of **2** that formed. The identities of the organic sulfonamide products were confirmed by comparison of their ¹H NMR spectra to those of authentic samples. Integration of the N–H signal of Pt(II)–sulfonamide **4a** indicated 29% conversion to **4a**, the Pt product of C–C reductive elimination. The Pt(II) species **2** and **4a** were the only products observed by ³¹P{¹H} NMR, and their identities were confirmed by comparison of their spectral data to that of independently synthesized complexes. Thus, 98% of the Pt is accounted for in the products (69% **2** and 29% **4a**). Similar reactivity and product ratios were observed for **1b** (65% yield of **2** and 35% yield of **4b**, 65% total yield of sulfonamides **3b** + **5b**). During the thermolysis of **1c** in C₆D₆, the methylsulfonamide product **3c** precipitated from solution preventing accurate integration and determination of yields.

Kinetic studies were performed in C₆D₆ at 100 °C to investigate the mechanism of C–N reductive elimination from **1a**. When the concentration data of **1a** as a function of time are subjected to a first-order kinetic treatment (ln([**1a**]₀/[**1a**]_t) vs *t*), it is seen that the plots are not linear (Figure 2). While the initial data appear linear through ca. 25% conversion, the plots curve downward, indicating that the reaction accelerates with time. The slope of the line through the early reaction times (25% conversion) gives an initial rate constant of *k*_{obs} = 1.1 × 10^{−5} s^{−1}. At the end of the reaction the *k*_{obs} value approaches 1.0 × 10^{−4} s^{−1}.

Compound **1a** was also thermolyzed at 100 °C in the polar solvent nitrobenzene-*d*₅. Exclusive C–C reductive elimination to form ethane and (dppbz)PtMe(NHSO₂(*p*-C₆H₄(CH₂)₃CH₃)) (**4a**) was observed under these conditions. This reaction was extremely fast at 100 °C; therefore, only an estimate of the rate was possible (*k*_{obs} = 4 × 10^{−3} s^{−1}). It should be noted, however, that the reaction in nitrobenzene-*d*₅ is 2 orders of magnitude faster than the thermolysis in C₆D₆.

Effect of Added Sulfonamides. The downward curve of the plot of ln([**1a**]₀/[**1a**]_t) vs time in C₆D₆ (Figure 2) suggests that a product of thermolysis could be responsible for the acceleration of the reaction. To investigate this possibility, the thermolysis

Scheme 2



of **1a** was carried out in the presence of added C–N coupled product **3a**. Thermolysis of **1a** in C_6D_6 at 100°C in the presence of 1–4 equiv of **3a** still resulted in curved first-order plots, but the curvature was much less pronounced. Thermolysis of **1a** with a large excess of **3a** (pseudo-first-order conditions, 9 mM **1a**, 150 mM **3a**) resulted in linear first-order kinetic behavior, with $k_{\text{obs}} = 3.6 \times 10^{-4} \text{ s}^{-1}$ (Figure 3).

Values of $k_{\text{obs}}(\text{initial})$ and $k_{\text{obs}}(\text{final})$ were extrapolated from the data in Figure 3, $k_{\text{obs}}(\text{initial})$ from the slope of the lines through the first 30% conversion and $k_{\text{obs}}(\text{final})$ from the slope of the lines through the final 30% conversion. The values of $k_{\text{obs}}(\text{initial})$ and $k_{\text{obs}}(\text{final})$ are provided in Table 2 for runs with and without added **3a**. These results are consistent with the observed nonlinear first-order kinetic behavior of the thermolysis of **1a** and support the proposal that production of **3a** during the thermolysis of **1a** leads to acceleration of the reaction.

Despite the faster reaction rate, the yields of the Pt(II) products **2** and **4a** in these reactions were roughly comparable to the yields obtained upon thermolyses of **1a** without added **3a**, with only a small increase in C–C coupling (ca. 5%) at the expense of C–N coupling. For example, **4a** was formed in a 35% yield and **2** was formed in a 64% yield upon thermolysis

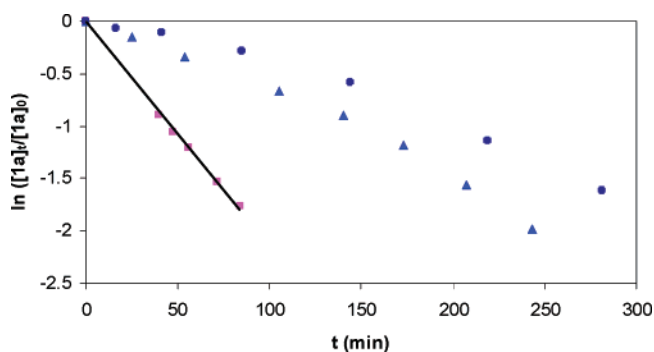


Figure 3. First-order kinetic plots for the thermolysis of **1a** in C_6D_6 at 100°C with added **3a** (● = 17 mM $[\mathbf{1a}]_0$, 20 mM $[\mathbf{3a}]_0$; ▲ = 9 mM $[\mathbf{1a}]_0$, 32 mM $[\mathbf{3a}]_0$; ■ = 9 mM $[\mathbf{1a}]_0$, 150 mM $[\mathbf{3a}]_0$).

Table 2. Rate Constants for Thermolysis of **1a** in C_6D_6 at 100°C , with and without Added **3a**

equiv of 3a	$k_{\text{obs}}(\text{initial})$ (10^4 s^{-1})	$k_{\text{obs}}(\text{final})$ (10^4 s^{-1})
0	0.11	0.96
1.2	0.55	1.3
3.6	1.0	1.9
17	N/A	3.6

of **1a** (9 mM) with 17 equiv of **3a** added, as compared to 29% and 69% without added **3a**. Notably, sulfonamide **5a** was not observed as a product of thermolysis when **3a** was added, and the amount of **3a** produced was consistent with the amount of **2** that formed.

The addition of sulfonamide **5a** to the reaction had an even greater accelerative effect than the addition of **3a** on the thermolysis of **1a**. When the thermolysis of **1a** in C_6D_6 at 100°C was carried out with 4.1 equiv of added **5a**, the reaction was complete in less than 1 h and occurred so quickly that only an estimate of the rate constant was possible ($k_{\text{obs}} \approx 1 \times 10^{-3} \text{ s}^{-1}$). The greater accelerative effect that sulfonamide **5a** has on the rate of thermolysis of **1a** provides an explanation for the observation that the $k_{\text{obs}}(\text{final})$ for thermolysis of **1a** alone ($9.6 \times 10^{-5} \text{ s}^{-1}$) was greater than the $k_{\text{obs}}(\text{initial})$ for thermolysis with 1.2 equiv of added **3a** ($5.5 \times 10^{-5} \text{ s}^{-1}$), as **5a** is formed as a byproduct in 18% yield during the thermolysis of **1a**.²⁰

Effect of Added Sulfonamide Anion. The thermolysis of **1a** in C_6D_6 ($[\mathbf{1a}]_0 = 5 \text{ mM}$) was also studied in the presence of sulfonamide anion, added as [K-18-crown-6][NHSO₂(*p*-C₆H₄(CH₂)₃CH₃)] (**6a**). The crown ether was employed to increase the solubility of the potassium salt of the sulfonamide in the nonpolar benzene solvent. Sulfonamide salt concentrations ranged from 1.5 to 15 mM. In each case, at the conclusion of the thermolysis, the Pt(II) product of C–N coupling, the Pt(II) product of C–C coupling, (dppbz)PtMe₂ (**2**), was detected in >95% yield (as determined by ¹H NMR) and was the only product observed by ³¹P NMR. Notably, ethane and (dppbz)PtMe(NHSO₂(*p*-C₆H₄(CH₂)₃CH₃)) (**4a**), the expected products of C–C reductive elimination, were not observed in these reactions.

Kinetic plots of $\ln([\mathbf{1a}]_t/[\mathbf{1a}]_0)$ versus time for the thermolyses carried out in C_6D_6 at 100°C in the presence of **6a** still exhibited downward curvature indicating acceleration of the reactions as the reactions progressed. However, the degree of curvature was significantly less than that found for the reactions without added **6a**. In addition, the degree of curvature of the plots decreased with higher concentrations of **6a**. An overlay plot of two kinetic experiments with concentrations of **6a** that differ by nearly an order of magnitude (1.5 mM vs 12 mM) clearly shows that the initial rate of reaction is not affected by the concentration of **6a** (Figure 4). The first-order plot of thermolysis of **1a** with the highest concentration of added **6a** (12 mM) appeared linear

(20) The unsubstituted sulfonamide **5a** is not observed during the thermolysis of **1a** with added **3a**.

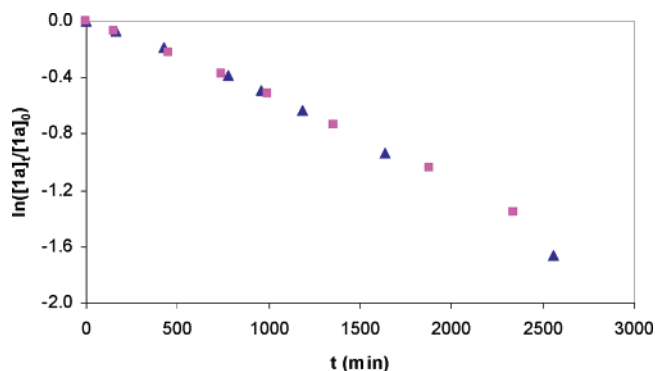
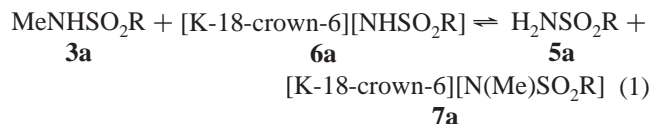


Figure 4. First-order kinetics plots for thermolysis of **1a** ($[1a]_0 = 5$ mM) in the presence of **6a** in C_6D_6 at 100 °C ($\blacktriangle = 1.5$ mM [**6a**]; $\blacksquare = 12$ mM [**6a**]).

through at least 30% conversion, and the slope of the line through these points gave an estimate of the initial rate constant for C–N reductive elimination of $k_{obs}(C-N) = 8.3 \times 10^{-6} s^{-1}$. This value agrees closely with the $k_{obs}(initial) = 1.1 \times 10^{-5} s^{-1}$ when no **6a** was added and both C–C and C–N reductive elimination reactions were observed.

The yield of the organic product of C–N coupling (**3a**) was challenging to establish in the presence of excess sulfonamide anion. Sulfonamide **3a** reacts with the added **6a** to form an equilibrium mixture with $H_2NSO_2(p-C_6H_4(CH_2)_3CH_3)$ (**5a**) and [K-18-crown-6] $[N(Me)SO_2(p-C_6H_4(CH_2)_3CH_3)]$ (**7a**), as shown in eq 1. This equilibration has been verified in independent experiments wherein **3a** and **6a** were combined in C_6D_6 solvent.



$$R = p-C_6H_4(CH_2)_3CH_3$$

The 1H NMR spectrum of a prepared mixture of **3a** and **6a** in C_6D_6 shows only one broad N–H resonance for **3a**, **5a**, and **6a** together, along with a single *N*-methyl resonance arising from the methyl groups on **3a** and **7a**. The remaining resonances in the 1H NMR spectrum result from the protons on the aryl rings and *n*-butyl chains of **3a**, **5a**, **6a**, and **7a**, and these signals overlap with one another making integration of resonances corresponding to each individual compound impossible. The total amount of **3a** and **7a** present after thermolysis was determined by integration of the *N*-bound methyl resonance, and these products together were consistently formed in 70% yield. A third sulfonamide product, $Me_2NSO_2(p-C_6H_4(CH_2)_3CH_3)$ (**8a**), was produced in 10% yield. Sulfonamide **8a** is not involved in the exchange reaction (eq 1) and can be quantified by integration of its distinct *N*-Me resonance (δ 2.27) in the 1H NMR spectrum. The value of the integral of the combined N–H resonance (**3a**, **5a**, and **6a**) upon completion of the thermolysis equals the sum of the integrals of the N–H-containing species (**1a** and **6a**) prior to thermolysis, indicating that sulfonamide mass balance is maintained.

A crossover experiment provided evidence that sulfonamide anion exchange at the Pt(IV) center occurs at lower temperatures than reductive elimination from complexes **1a,b**. The tolylsulfonamide complex **1b** (12.3 mM) was heated at 85 °C in C_6D_6 in the presence of the *n*-butylbenzenesulfonamide salt **6a** (13.3

mM, 1.08 equiv). After 25 h, complete sulfonamide exchange was evident, resulting in an equilibrium mixture of **1b**, **6a**, **1a**, and **6b** (Scheme 3). Overlap of signals in the 1H NMR prevented an accurate determination of the equilibrium constant. A small amount ($\sim 5\%$) of the Pt(II) product **2**, resulting from C–N reductive elimination, was also observed to form at this temperature during the 25 h period.

Effect of Added Water. Thermolysis samples were prepared using dry solvents under rigorously air-free conditions with oven-dried NMR tubes that were flame-sealed under vacuum. It was noted, however, that although no water was detected in the 1H NMR spectra of **1a** in C_6D_6 prior to thermolysis, trace amounts of water were observed after heating. For this reason, the effect of additional water on the thermolysis reactions was probed and the thermolysis of **1a** was carried out in undried C_6D_6 rather than in C_6D_6 that had been vacuum transferred from sodium. Integration of the H_2O resonance in the 1H NMR spectrum prior to thermolysis indicated an approximate 1:1 ratio of water to **1a**. In this thermolysis reaction with water present, the C–C reductive elimination pathway was the dominant decomposition pathway, with 64% formation of $(dppbz)PtMe-(NH\text{SO}_2(p-C_6H_4(CH_2)_3CH_3))$ (**4a**) and 33% formation of $(dp-pbz)PtMe_2$ (**2**) as observed by 1H and ^{31}P NMR. Despite the 33% yield of **2**, the C–N-coupled sulfonamide product **3a** formed in a modest 15% yield. The yield of $H_2NSO_2(p-C_6H_4(CH_2)_3CH_3)$ (**5a**) was 20% in this reaction, making **5a** the dominant organic sulfonamide product. Notably, the yield of methanol increased to 17%. Again, the sum of the yields of **3a** and **5a** are equivalent to the amount of **2** formed. An additional thermolysis reaction was carried out in which water (0.006 mmol) was added to a sample of **1a** (0.004 mmol) in dry C_6D_6 (0.4 mL) via vacuum transfer, and the results were nearly identical. Although kinetics data were not recorded for the thermolyses of **1a** with additional water, these reactions qualitatively occurred much faster than thermolyses of **1a** in dry C_6D_6 and reached completion within 8 h.

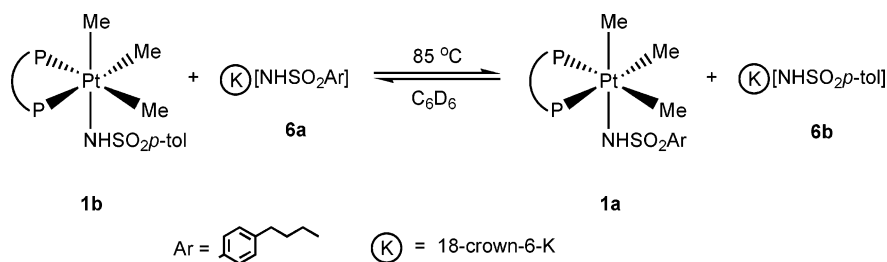
Synthesis and Reactivity of *fac*-(*dppbz*)PtMe₃(*N*(Me)SO₂(*p*-C₆H₄(CH₂)₃CH₃)) (9a). Compound **9a**, the *N*-methyl analogue of **1a**, was prepared in situ by the deprotonation of **1a** with KH in THF followed by addition of iodomethane and filtration to remove the KI precipitate (Scheme 4). The 1H NMR data for **9a** are similar to that for **1a**, with the exception of the N–H resonance, which is replaced by an N–Me singlet resonance at 2.76 ppm, broadened at the base due to Pt–H coupling ($^3J_{Pt-H} \approx 11$ Hz). The absence of this peak in the spectrum of **9a-d₃**, prepared by the addition of CD_3I rather than CH_3I , supports the assignment of the N–Me resonance.

Compound **9a** was unstable in solution at room temperature and decomposed slowly overnight upon standing in benzene or THF to the Pt(II) products $(dppbz)PtMe_2$ (**2**) (ca. 75%) and $(dppbz)PtMe(N(Me)SO_2(p-C_6H_4(CH_2)_3CH_3))$ (ca. 25%), as observed by ^{31}P NMR. The organic products of this decomposition were ethane, methane, and an unusual sulfonamide dimer, $CH_2-(N(Me)SO_2(p-C_6H_4(CH_2)_3CH_3))_2$ (**10a**).²¹ The known Pt(IV)–hydride *fac*-(*dppbz*)PtMe₃H²² was detected as a transient intermediate (^{31}P NMR, 25 ppm; 1H NMR Pt–H, –8.2 ppm, $^1J_{Pt-H} = 687$ Hz).

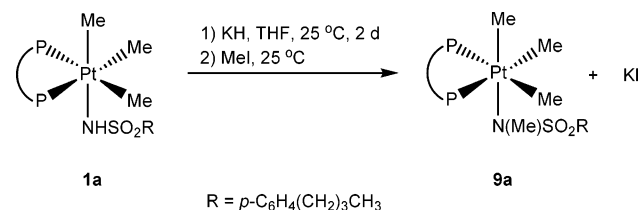
(21) Sekera, A.; Rumpf, P. C. *R. Acad. Sci.* **1965**, *260*, 2252.

(22) Crumpton-Bregel, D. M.; Goldberg, K. I. *J. Am. Chem. Soc.* **2003**, *125*, 9442.

Scheme 3



Scheme 4



Attempts to prepare **9a** via a condensation route similar to that shown in Scheme 1 were unsuccessful. When *fac*-(dppbz)-PtMe₃(OH) was allowed to react with an excess of **3a** in C₆D₆, compound **9a** was detected in small amounts at early reaction times but rapidly decomposed to the same products mentioned above. The Pt(IV)-hydride *fac*-(dppbz)PtMe₃H was also observed in these reactions as an intermediate decomposition product by both ³¹P and ¹H NMR.

Heating a solution of the *N*-methylsulfonamide complex **9a** in C₆D₆ at 100 °C for only 30 min resulted in complete conversion to (dppbz)PtMe₂ (**2**), as observed by ³¹P and ¹H NMR spectroscopy. Integration of the Pt–Me signal of **2** in the ¹H NMR spectrum indicated >93% conversion to this product. The only organic products of this reaction identified in the ¹H NMR spectrum were the sulfonamide dimer **10a** (40% yield),²³ methane, and dimethylsulfonamide **8a** (30–40% yield) (Scheme 5). Compound **8a** is the sulfonamide product resulting from C–N reductive elimination from **9a**. In contrast to the slow room-temperature decomposition, no products resulting from C–C reductive elimination are observed upon thermolysis. Although the Pt(II) product **2** was consistently formed in >90% yield, the total yield of the organic products **10a** and **8a** only accounted for approximately 80% of the sulfonamide moiety. However, no additional resonances were observed in the ¹H NMR spectrum after thermolysis and no additional products were detected by GC/MS.

Compound **9a-d₃** was thermolyzed under the same conditions, and selective deuterium incorporation into the identified organic products was observed. The partially deuterated dimer (RO₂-SN(CH₃)CD₂(N(CD₃)SO₂R) (**10a-d₅**) was formed, along with CH₃D as the only isotopomer of methane and CH₃N(CD₃)SO₂R (**8a-d₃**) (R = *p*-C₆H₄(CH₂)₃CH₃) (Scheme 5). Again, the only Pt product observed was **2**.

Discussion

Mechanism of C–N Reductive Elimination from 1a. There are very few examples of reductive elimination reactions to form carbon(sp³)–heteroatom bonds from metal centers.^{6–8,10,11,24,25} However, since this could potentially be a very powerful reaction

if incorporated as the product forming step in catalytic reactions, the discovery of new examples of this reactivity in model systems provides a tremendous opportunity to gain understanding of the mechanism of such couplings and how to promote them. The results of previously reported mechanistic studies of alkyl C–I and alkyl C–O reductive eliminations from Pt(IV) complexes *fac*-L₂PtMe₃X (L₂ = dppe, dppbz; X = iodide, carboxylate, or aryloxy) support a common two-step mechanism for both C–O and C–I bond formation.^{10,11} In the first step, dissociation of X[–] from the Pt(IV) center forms the cationic five-coordinate intermediate [L₂PtMe₃]⁺. An S_N2 nucleophilic attack by X[–] on a Pt-bound methyl group of this intermediate forms the C–X-coupled product and the Pt(II) species L₂PtMe₂. An analogous mechanism for the C–N reductive elimination from **1** (path D, Scheme 6) is considered here, as well as three additional possible mechanisms (Scheme 6).

Path A is presented as a two-step mechanism in Scheme 6, but the two steps could also occur simultaneously. In the first step, sulfonamide anion acts as a nucleophile to attack a methyl group of the six-coordinate Pt(IV) starting complex to form the methylsulfonamide product **3a** and an anionic, five-coordinate Pt(II) intermediate. Loss of sulfonamide anion from this intermediate affords the Pt(II) product (dppbz)PtMe₂ (**2**). This mechanism should exhibit a direct first-order dependence upon [NHSO₂R[–]]. However, the rate of C–N reductive elimination from **1a** was found to be independent of the concentration of added sulfonamide anion in direct conflict with this pathway.

None of the remaining mechanistic pathways should show a dependence on sulfonamide anion concentration. In path B, dechelation of one end of the dppbz ligand affords a neutral five-coordinate intermediate which then undergoes C–N bond formation to form **3a**, followed by recoordination of the phosphine ligand to form **2**. A similar mechanism has been reported for C–C reductive elimination from (dppe)PtMe₄,²² and it was recently proposed that the mechanism of C(sp²)–O reductive elimination from Pd(IV) complexes containing cyclometalated pyridine ligands proceeds through a neutral five-coordinate intermediate formed by the dissociation of a pyridyl nitrogen of a bidentate ligand.²⁶ Direct reductive elimination of CH₃I from neutral, five-coordinate Rh(III) pincer complexes was also recently reported.²⁷

In pathway C, C–N reductive elimination occurs directly from the coordinatively saturated starting material **1a**. Direct

(23) The dimer **10a** contains two sulfonamide moieties and forms from 2 equiv of the starting material **1a**.

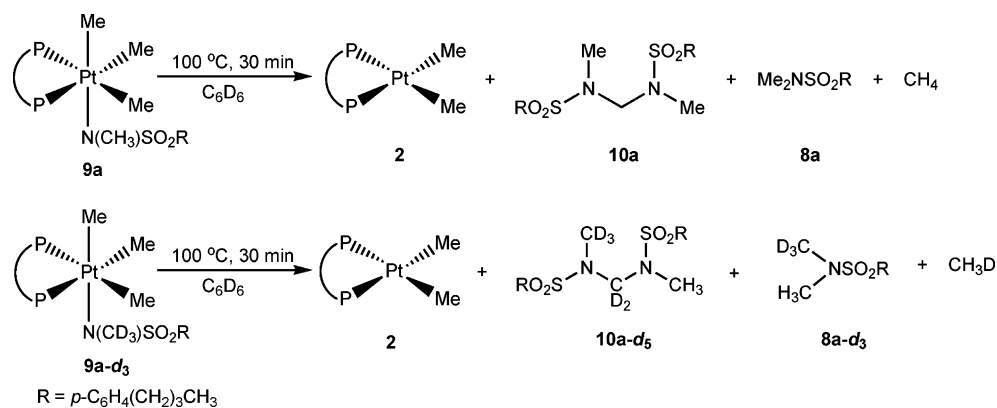
(24) Matsunaga, P. T.; Hillhouse, G. L. *J. Am. Chem. Soc.* **1993**, *115*, 2075.

(25) (a) Luinstra, G. A.; Labinger, J. A.; Bercaw, J. E. *J. Am. Chem. Soc.* **1993**, *115*, 3004. (b) Hutson, A. C.; Lin, M.; Basickes, N.; Sen, A. *J. Organomet. Chem.* **1995**, *504*, 69. (c) Luinstra, G. A.; Wang, L.; Stahl, S. S.; Labinger, J. A.; Bercaw, J. E. *J. Organomet. Chem.* **1995**, *504*, 75. (d) Stahl, S. S.; Labinger, J. A.; Bercaw, J. E. *Angew. Chem., Int. Ed.* **1998**, *37*, 2180. (e) Vedernikov, A. N.; Binfield, S. A.; Zavalij, P. Y.; Khusnutdinova, J. R. *J. Am. Chem. Soc.* **2006**, *128*, 82.

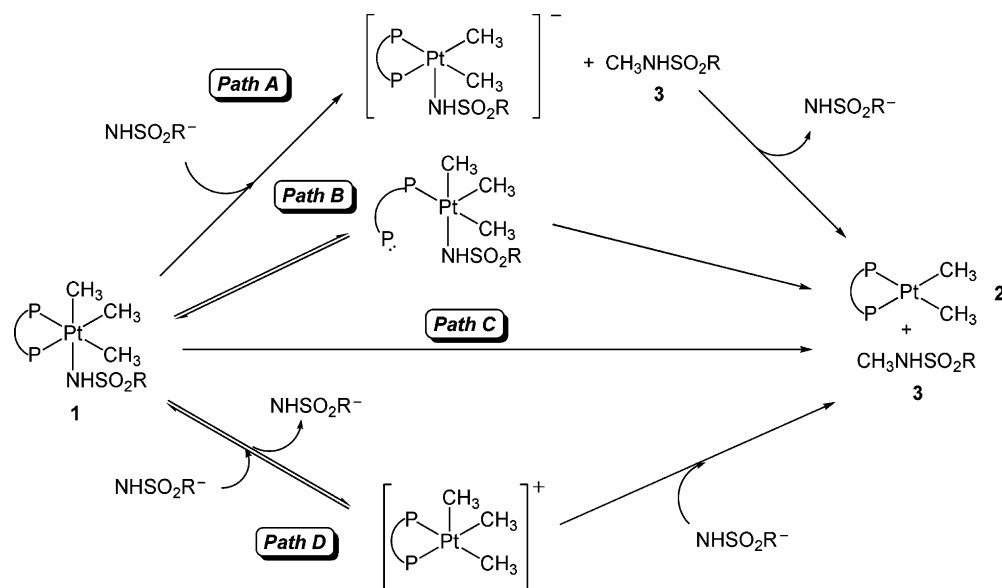
(26) Dick, A. R.; Kampf, J. W.; Sanford, M. S. *J. Am. Chem. Soc.* **2005**, *127*, 12790.

(27) Frech, C. M.; Milstein, D. *J. Am. Chem. Soc.* **2006**, *128*, 12434.

Scheme 5



Scheme 6



reductive elimination from six-coordinate Pt(IV) is feasible but appears to be quite rare. In virtually all studies of reductive elimination to form C–H, C–C, and C–X bonds from Pt(IV) or Pd(IV), the formation of five-coordinate intermediates prior to the reductive coupling has been indicated.^{10,11,22,26–28} Notably, however, in the study of C–H reductive elimination to form methane from *fac*-L₂PtMe₃H (L₂ = dppe, dppbz), mechanistic investigations supported a direct pathway, one without preliminary ligand dissociation.²²

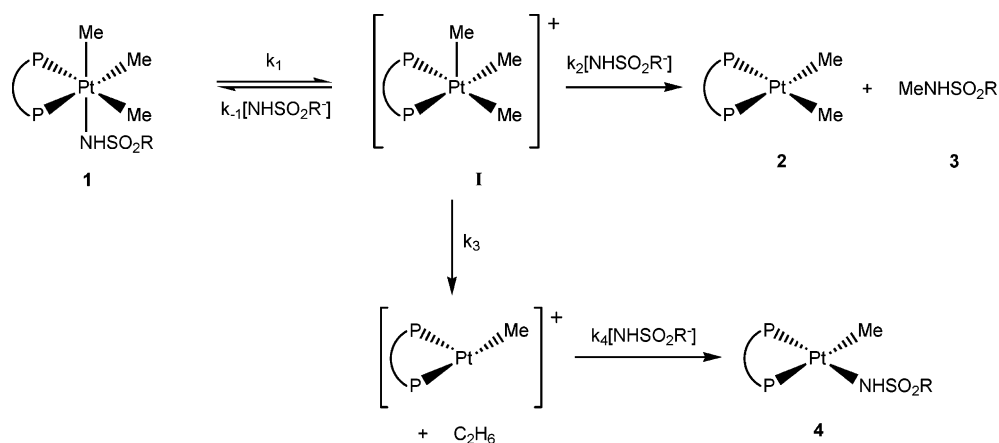
In path D, dissociation of NHSO₂R[−] from **1a** occurs to form a cationic five-coordinate intermediate. Nucleophilic attack by the dissociated sulfonamide anion at a methyl group on the five-coordinate Pt(IV) cation generates sulfonamide **3a** and (dppbz)PtMe₂ (**2**). This pathway is analogous to the accepted mechanism for C–O and C–I reductive elimination from the closely related Pt(IV) complexes *fac*-L₂PtMe₃X (L₂ = dppe, dppbz; X = iodide, carboxylate, or aryloxy).^{10,11} Although path D requires NHSO₂R[−] to act as a nucleophile to form the C–N bond in the rate-determining step, the rate of the reductive elimination reaction should be independent of [NHSO₂R[−]].²⁹

While paths B–D are not expected to show dependence on sulfonamide anion concentration, only path D should be significantly affected by added sulfonamide product **3a**. The sulfonamide product **3a** can act as a Lewis acid to facilitate the dissociation of NHSO₂R[−] from **1a**. Acetic acid and phenols were found to act in this manner and accelerate C–O reductive elimination from *fac*-L₂PtMe₃(OR) (R = C(O)Me, Ar) complexes.¹⁰ Indeed, added sulfonamide **3a** was shown to accelerate the C–N reductive elimination reaction from **1a**. Thus, reductive elimination to form **3a** would be expected to accelerate as more

(28) (a) Brown, M. P.; Puddephatt, R. J.; Upton, C. E. E. *J. Chem. Soc., Dalton Trans.* **1974**, 2457. (b) Roy, S.; Puddephatt, R. J.; Scott, J. D. *J. Chem. Soc., Dalton Trans.* **1989**, 2121. (c) Hill, G. S.; Yap, G. P. A.; Puddephatt, R. J. *Organometallics* **1999**, *18*, 1408. (d) Byers, P. K.; Cauty, A. J.; Crespo, M.; Puddephatt, R. J.; Scott, J. D. *Organometallics* **1988**, *7*, 1363. (e) Aye, K. T.; Cauty, A. J.; Crespo, M.; Puddephatt, R. J.; Scott, J. D.; Watson, A. A. *Organometallics* **1989**, *8*, 2709. (f) Cauty, A. J. *Acc. Chem. Res.* **1992**, *25*, 83. (g) van Asselt, R.; Rijnberg, E.; Elsevier, C. J. *Organometallics* **1994**, *13*, 706. (h) Markies, B. A.; Cauty, A. J.; Boersma, J.; van Koten, G. *Organometallics* **1994**, *13*, 2053. (i) Ducker-Benfer, C.; van Eldik, R.; Cauty, A. J. *Organometallics* **1994**, *13*, 2412. (j) Cauty, A. J. In *Comprehensive Organometallic Chemistry*, 2nd ed.; Puddephatt, R. J., Ed.; Pergamon: New York 1995; Vol. 9, Chapter 5. (k) Kruis, D.; Markies, M. A.; Cauty, A. J.; Boersma, J.; van Koten, G. *J. Organomet. Chem.* **1997**, *532*, 235. (l) Cauty, A. J.; Hoare, J. L.; Davies, N. W.; Traill, P. R. *Organometallics* **1998**, *17*, 2046. (m) Cauty, A. J.; Hoare, J. L.; Patel, J.; Pfeffer, M.; Skelton, B. W.; White, A. H. *Organometallics* **1999**, *18*, 2660. (n) Bayler, A.; Cauty, A. J.; Edwards, P. G.; Skelton, B. W.; White, A. H. *J. Chem. Soc., Dalton Trans.* **2000**, 3325. (o) Puddephatt, R. J. *Angew. Chem., Int. Ed.* **2002**, *41*, 261. (p) Procelewska, J.; Zahl, A.; Liehr, G.; van Eldik, R.; Smythe, N. A.; Williams, B. S.; Goldberg, K. I. *Inorg. Chem.* **2005**, *44*, 7732.

(29) The rate law for the C–N reductive elimination reaction pathway shown in Scheme 7 (also path D, Scheme 6) simplifies to the following: rate = $k_{C-N}[\mathbf{1a}]$, where $k_{C-N} = (k_1k_2)/(k_2 + k_{-1})$. This rate law is independent of [NHSO₂R[−]]. See ref 10.

Scheme 7



3a is produced, and such behavior is clearly evident in the downward curvature of the first-order kinetic plots of the reaction. While such accelerative behavior is expected if the reaction proceeds by path D, it is difficult to rationalize the accelerative effect of methylsulfonamide **3a** on the rate of reaction for either the phosphine dissociation mechanism (path B) or direct reductive elimination from **1a** (path C).

Note that while a hydrogen-bonding interaction between the methylsulfonamide product **3a** and the sulfonamide moiety of **1a** would be expected to facilitate sulfonamide dissociation from **1a**, such an interaction should also be expected to decrease the nucleophilicity of the resulting sulfonamide anion. The overall acceleration in the C–N reductive elimination results from a larger influence of the hydrogen bonding on the preequilibrium step. This is similar to the observation of a positive ρ value for the overall C–O reductive elimination of methyl aryl ethers from *fac*-L₂PtMe₃(OR) which results from the sum of a large positive equilibrium ρ value for OAr[−] dissociation and a smaller negative kinetic ρ value for nucleophilic attack at the C(sp³) by the OAr[−] group.^{10b}

The mechanism in path D is also supported by the results of the sulfonamide anion-exchange reaction. It was shown that the exchange of sulfonamide anion is significantly more rapid than the C–N reductive elimination. Complete exchange with added sulfonamide was observed (i.e., equilibrium was reached) at 85 °C, 15 °C lower than the temperature at which reductive elimination was studied (Scheme 3). Sulfonamide anion exchange by an associative mechanism at Pt(IV) seems unlikely, and thus, this result supports the kinetic viability of sulfonamide dissociation as a preequilibrium first step under the reaction conditions.

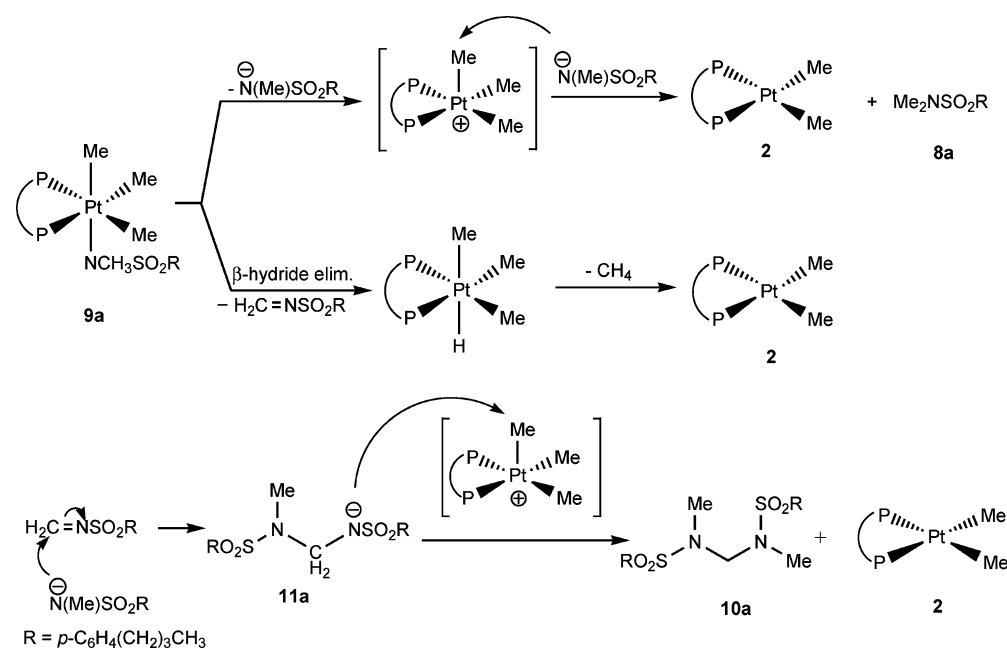
When the thermolysis of **1a** is carried out without added sulfonamide anion, carbon–carbon coupling to form ethane is competitive with the C–N reductive elimination to produce **3a**. A competing C–C reductive elimination was also observed with C–X reductive elimination from the Pt(IV) complexes *fac*-L₂-PtMe₃X (L₂ = dppe, dppbz; X = iodide, carboxylate, or aryloxy). In these systems, the C–C coupling occurs from the same cationic five-coordinate intermediate as the C–X coupling.^{10,11} The complete inhibition of the C–C coupling reaction in the presence of added sulfonamide anion implies a similar mechanism for ethane production from **1a**. The results of the kinetic and mechanistic studies described above are all fully consistent with the mechanism shown in Scheme 7

for C–N and C–C reductive elimination from **1a**. Initial dissociation of sulfonamide anion occurs to form the intermediate five-coordinate Pt(IV) cation **I**. Nucleophilic attack by NHSO₂R[−] at a methyl group of **I** forms the C–N-coupled product **3a** and the Pt(II) product **2**. C–C reductive elimination of ethane occurs directly from **I**, and the resulting unsaturated Pt(II) species is trapped by NHSO₂R[−] to yield **4**. In the presence of added NHSO₂R[−], C–C reductive elimination from **I** is inhibited as the rate of nucleophilic attack on intermediate **I** ($k_2[\text{NHSO}_2\text{R}^-][\text{I}]$) becomes larger than that of C–C coupling ($k_3[\text{I}]$).

The mechanism shown in Scheme 7 also provides a rationale for the observed solvent dependence of the product distribution. Although C–N reductive elimination from **1** is favored in the nonpolar solvent C₆D₆, use of the polar solvent nitrobenzene-*d*₅ enhances the C–C coupling pathway and no C–N coupling is observed. The polar solvent nitrobenzene should favor the formation of the five-coordinate cationic intermediate, the first step in both pathways. However, the second step of C–N reductive elimination should be less favored in polar solvents as the charged intermediates are partially neutralized in the transition state. As a result, the rate of the C–C reductive elimination reaction increases more significantly with the polarity of the solvent than that of C–N reductive elimination and C–C reductive elimination is the exclusive pathway in the very polar nitrobenzene solvent. Similar solvent effects were seen in the product distributions and relative rates of C–O and C–C couplings from *fac*-L₂PtMe₃(OR) complexes.¹⁰

Finally, the competitive mechanism depicted in Scheme 7 is also consistent with the faster rates of reactions observed for thermolyses of **1a** carried out with added sulfonamide **3a** and with added water. Both of these additives can act as Lewis acids to promote the first step of both C–N and C–C reductive elimination—the dissociation of NHSO₂R[−]. While this interaction of sulfonamide **3a** with the sulfonamide anion would be expected to slow the second step of C–N reductive elimination (the nucleophilic attack of NHSO₂R[−] on the Pt(IV)–Me of **I**), the larger contribution to the equilibrium first step results in a faster C–N reductive elimination (see above). In contrast, the C–C reductive elimination only experiences the increase in the rate of the first step and so the C–C reductive elimination rate might be expected to increase more than the C–N reductive elimination rate. Indeed, a small increase in the amount of C–C-coupled product (from 29% to 35%) was observed

Scheme 8



at the expense of C–N-coupled product in the presence of 17 equiv of **3a**. The effect of the added water on the product ratio was more dramatic, as C–C reductive elimination increased from 29% to 64% in the presence of 1 equiv of H₂O. There was relatively little C–N coupling to produce **3a** (15%) as the major sulfonamide containing product was **5a**, consistent with protonation of the dissociated sulfonamide anion by the water.

Decomposition of 9a. Compound **9a**, the *N*-methyl derivative of **1a**, was less stable in C₆D₆ solution than **1a**, and complete decomposition of **9a** to the Pt(II) compound **2** was observed within 30 min upon thermolysis at 100 °C, forming dimethylsulfonamide **8a** from C–N reductive elimination, as well as the sulfonamide dimer **10a** and methane as organic products (Scheme 5). Slow room-temperature decomposition of **9a** formed the same products in addition to small amounts of ethane and (dppbz)PtMe(N(Me)SO₂(*p*-C₆H₄(CH₂)₃CH₃)), the products of C–C reductive elimination from **9a**. Monitoring the room-temperature decomposition of **9a** by ¹H and ³¹P NMR allowed for the observation of the Pt(IV)–hydride *fac*-(dppbz)PtMe₃H²² as an intermediate. Compound **9a** differs from **1a** in that it is susceptible to β-hydride elimination because of the methyl group on nitrogen. β-hydride elimination is a common decomposition pathway for late-metal alkylamides.^{16a} β-hydride elimination from **9a** would form the *N*-sulfonylimine species H₂C=NSO₂-(*p*-C₆H₄(CH₂)₃CH₃), which was not directly observed, and Pt(IV)-hydride *fac*-(dppbz)PtMe₃H, which was observed and is known to react further under these conditions to form the observed products of methane and (dppbz)PtMe₂ (**2**).²² The terminal methylene carbon of the *N*-sulfonylimine is expected to be highly electrophilic,³⁰ and reaction with methylsulfonamide anion N(Me)SO₂R[−] would form the new anion **11a**. Nucleophilic attack on a Pt(IV) methyl group by anion **11a** can then form the observed sulfonamide dimer **10a** (Scheme 8).

Isotopic labeling experiments provide support for this unusual decomposition pathway. The labeled compound **9a**-*d*₃ decom-

poses to the same products as **9a**, with deuterium partially incorporated into **8a** and **10a** to form **8a**-*d*₃ and **10a**-*d*₅ (Scheme 5). CH₃D is the only isotopomer of methane that is observed, consistent with the formation of *fac*-(dppbz)PtMe₃D by β-deuteride elimination. Support for the formation of the reactive deuterated sulfonylimine intermediate is provided by the incorporation of deuterium into the methylene bridge of dimer **10a**-*d*₅. That one methyl group of both products **8a** and **10a** remains undeuterated is consistent with the proposed nucleophilic attacks on the five-coordinate Pt cation (Scheme 8).

It is noteworthy that the classical mechanism for β-hydride elimination requires the presence of a vacant coordination site cis to the metal alkyl, alkoxide, or alkylamine.^{9a} However, there is evidence in related Pt(IV) systems to support that the rigid ancillary dppbz ligand is not likely to dissociate under the thermolysis conditions.²² Thus, the absence of facile access to an empty coordination site cis to the sulfonamide ligand in **9a** appears in conflict with a proposal of β-hydride elimination. However, examples of nonclassical β-hydride elimination reactions for transition metal alkoxides have been reported.^{31–33} The data from two of these systems are consistent with dissociation of the alkoxide to generate the open site that accommodates the transfer of the hydride from the alkoxide to the metal.^{32,33} A similar mechanism is proposed for this Pt(IV) system where considerable evidence for dissociation of the sulfonamide anion has been presented. The observation of *fac*-(dppbz)PtMe₃H as an intermediate is consistent with this proposal.

Formation of Additional Sulfonamide Products. Thermolysis of **1a** in C₆D₆ in the presence of the sulfonamide salt **6a** produces sulfonamides **3a** and **5a**, with formation of dimethylsulfonamide **8a** in small amounts as well. The formation of **8a** can be rationalized by the equilibrium shown in eq 1. Reaction of methylsulfonamide product **3a** with the anion of **6a** forms H₂NSO₂(*p*-C₆H₄(CH₂)₃CH₃) (**5a**) and the methylsulfonamide anion of **7a** (eq 1). The methylsulfonamide anion of

(31) Ritter, J. C. M.; Bergman, R. G. *J. Am. Chem. Soc.* **1998**, *120*, 6826.

(32) Blum, O.; Milstein, D. *J. Organomet. Chem.* **2000**, *593–594*, 479.

(33) Farad, C. M.; Ozerov, O. V. *Inorg. Chim. Acta* **2007**, *360*, 286.

(30) Bharatam, P. V.; Kaur, A.; Kaur, D. *Tetrahedron* **2002**, *58*, 10335.

7a can nucleophilically attack a methyl group on the five-coordinate intermediate to form **8a** and **2**, as proposed in the top reaction in Scheme 8 for the formation of $\text{Me}_2\text{NSO}_2(p\text{-C}_6\text{H}_4(\text{CH}_2)_3\text{CH}_3)$ upon thermolysis of **9a**.

Notably, the dimethylsulfonamide product **8a** is only observed during thermolysis of **1a** in the presence of added sulfonamide salt **6a**. Thermolysis of **1a** alone produces only the expected product **3a** and the unsubstituted sulfonamide **5a** as the organic sulfonamide products. Small amounts of methanol (<5%) also formed upon thermolysis of **1a**. The yields of **3a** and **5a** together equaled the amount of the corresponding Pt(II) product **2** that was formed. In these reactions, adventitious water in the NMR could be responsible for the formation of **5a** and of the methanol. Despite handling of the samples under rigorously air- and moisture-free conditions, trace amounts of water are observed in the ^1H NMR spectra of **1a** upon heating. The first step of the mechanism of reductive elimination from **1a** is the dissociation of NHSO_2R^- from the platinum center to form the five-coordinate intermediate. Any water in the sample could assist in the dissociation and react with the dissociated anion to form **5a** and hydroxide anion. Reaction of the hydroxide anion with the five-coordinate intermediate would form **2** and methanol. Consistent with this proposal, the yields of both methanol and sulfonamide **5a** increased significantly upon addition of water to the thermolysis reactions.

Conclusions

The novel Pt(IV)–sulfonamide complexes $\text{fac}(\text{dppbz})\text{PtMe}_3(\text{NHSO}_2\text{R})$ ($\text{R} = p\text{-C}_6\text{H}_4(\text{CH}_2)_3\text{CH}_3, p\text{-C}_6\text{H}_4\text{CH}_3, \text{CH}_3$) (**1a–c**) were prepared from $\text{fac}(\text{dppbz})\text{PtMe}_3(\text{OH})$ and the corresponding sulfonamide in THF at room temperature. These complexes undergo C–N reductive elimination upon thermolysis in C_6D_6 to form methylsulfonamides **3a–c** in high yield. C–C coupling also occurs to form ethane and Pt(II)–sulfonamides **4a–c** in lower yield. High selectivity for the C–N reductive elimination pathway can be achieved by addition of sulfonamide anion to the thermolysis reactions. These C–N reductive elimination reactions represent the first examples of directly observed thermal $\text{C}(\text{sp}^3)\text{–N}$ reductive elimination. Mechanistic studies of the thermolysis of **1a** support a two-step reaction pathway of initial dissociation of NHSO_2R^- from the metal center to form a cationic five-coordinate intermediate, followed by nucleophilic attack by NHSO_2R^- on a methyl group of this intermediate to form the products. This mechanism is analogous to the mechanisms for C–O and C–I reductive eliminations reported from similar Pt(IV) complexes.^{10,11} Thus, an apparently general mechanism for $\text{C}(\text{sp}^3)\text{–I}$, $\text{C}(\text{sp}^3)\text{–O}$, and $\text{C}(\text{sp}^3)\text{–N}$ reductive elimination from Pt(IV) has been identified. Also significant is that the second step of this mechanism, the nucleophilic attack of the X group on the alkyl group of a five-coordinate d^6 metal, is similar to that observed in C–O and C–X bond-forming reactions at Pt(IV)^{10,11,25} and at Rh(III).⁸ Thus, in all these cases, the rare alkyl C–X coupling step occurs via a common mechanism of nucleophilic attack of the heteroatom group at a high-valent d^6 five-coordinate alkyl species. This apparent generality of the mechanism of alkyl carbon–heteroatom bond formation from high-valent d^6 metal centers should be of significant use in the design of catalysts for organic transformations relying on the challenging formation of an alkyl carbon–heteroatom bond.

Experimental Section

General Comments. Unless otherwise noted, all manipulations were carried out under a nitrogen atmosphere in a drybox or using standard vacuum-line techniques. Tetrahydrofuran, benzene, benzene- d_6 , toluene, and diethyl ether were transferred under vacuum from sodium/benzophenone. Pentane was transferred from CaH_2 . Iodomethane (Strem) was dried with and stored under 4 Å molecular sieves. KH was purchased from Aldrich as a suspension in oil and was filtered under nitrogen and washed with hexanes prior to use. *o*-Bis(diphenylphosphino)benzene (Strem) was stirred with KH in THF and then recrystallized from THF/pentane. The Pt(IV) compounds $\text{fac}(\text{dppbz})\text{PtMe}_3(\text{O}_2\text{CCF}_3)$ ¹⁰ and $\text{fac}(\text{dppbz})\text{PtMe}_3(\text{OH})$ ¹⁵ were prepared as previously described. 4-*n*-Butylbenzenesulfonamide and 4-*n*-butylbenzenesulfonyl chloride were purchased from Alfa Aesar and used as received. All other reagents and solvents were purchased from Aldrich and used as received. NMR spectra were recorded using Bruker DRX 499, AV 500, AV 301, or DPX 200 spectrometers. ^1H NMR spectra were referenced to residual proton peaks in the deuterated solvent, and chemical shifts (δ) are reported in ppm relative to tetramethylsilane. $^{31}\text{P}\{^1\text{H}\}$ NMR spectra were referenced to an external standard of 85% H_3PO_4 .

Synthesis of $\text{fac}(\text{dppbz})\text{PtMe}_3(\text{NHSO}_2\text{R})$ (1a–c**).** The Pt(IV)–sulfonamide complexes were prepared from $\text{fac}(\text{dppbz})\text{PtMe}_3(\text{OH})$ and the corresponding sulfonamide in THF. For **1a**, $\text{fac}(\text{dppbz})\text{PtMe}_3(\text{OH})$ (75.8 mg, 0.108 mmol) and excess 4-*n*-butylbenzenesulfonamide (47.5 mg, 0.223 mmol) were dissolved in 10 mL of dry THF. The solution was stirred overnight. MgSO_4 was added as a drying agent and the reaction mixture stirred for 10 min and then filtered through a Teflon syringe filter. The solvent was removed from the filtrate under vacuum, and the oily solid residue was washed with cold Et_2O (2×5 mL) to remove excess sulfonamide. The remaining white solid was dried under vacuum overnight and recrystallized from THF/pentane to afford **1a** in a 65% isolated yield (63 mg). **1b,c** were prepared by analogous procedures. **1a**: ^1H NMR (C_6D_6) δ 0.32 (t w/Pt satellites, 3H, $^3J_{\text{P–H}} = 7.5$, $^2J_{\text{P–H}} = 67$, Pt– CH_3 trans to N), 0.84 (t, 3H, $^3J_{\text{H–H}} = 7.3$, $-\text{CH}_2\text{CH}_2\text{CH}_2\text{CH}_3$), 1.20 (m, 2H, $-\text{CH}_2\text{CH}_2\text{CH}_2\text{CH}_3$), 1.42 (m, 2H, $-\text{CH}_2\text{CH}_2\text{CH}_2\text{CH}_3$), 1.77 (br s, 1H, NH), 1.89 (vt w/Pt satellites, 6H, $^3J_{\text{P–H}} = 7.0$, $^2J_{\text{P–H}} = 60$, Pt– CH_3 cis to N), 2.45 (t, 2H, $^3J_{\text{H–H}} = 7.7$, $-\text{CH}_2\text{CH}_2\text{CH}_3$), 6.8–8.0 (m, 24H, protons of phosphine and sulfonamide aryl rings, unresolved); $^{31}\text{P}\{^1\text{H}\}$ NMR (C_6D_6) δ 17.9 (s w/Pt satellites, $^1J_{\text{P–P}} = 1028$). **1b**: ^1H NMR (THF- d_8) δ –0.09 (t w/Pt satellites, 3H, $^3J_{\text{P–H}} = 7.5$, $^2J_{\text{P–H}} = 66$, Pt– CH_3 trans to N), 1.23 (vt w/Pt satellites, 6H, $^3J_{\text{P–H}} = 7.0$, $^2J_{\text{P–H}} = 60$, Pt– CH_3 cis to N), 1.33 (s w/Pt satellites, 1H, $^2J_{\text{P–H}} = 1.5$, NH), 2.30 (s, 3H, $p\text{-C}_6\text{H}_4\text{CH}_3$), 7.0–7.7 (m, 24H, protons of phosphine aryl rings and *p*-tolyl group, unresolved); $^{31}\text{P}\{^1\text{H}\}$ NMR (THF- d_8) δ 15.9 (s w/Pt satellites, $^1J_{\text{P–P}} = 1030$). **1c**: ^1H NMR (THF- d_8) δ –0.10 (t w/Pt satellites, 3H, $^3J_{\text{P–H}} = 7.3$, $^2J_{\text{P–H}} = 65$, Pt– CH_3 trans to N), 1.27 (vt w/Pt satellites, 6H, $^3J_{\text{P–H}} = 6.5$, $^2J_{\text{P–H}} = 60$, Pt– CH_3 cis to N), 2.33 (s, 3H, HNSO_2CH_3), 7.2–7.8 (m, 20H, protons of phosphine aryl rings, unresolved) (signal for the NH proton of the Pt– NHSO_2Me group coincident with residual protio THF in the deuterated solvent (δ 1.4)); $^{31}\text{P}\{^1\text{H}\}$ NMR (THF- d_8) δ 16.3 (s w/Pt satellites, $^1J_{\text{P–P}} = 1044$).

X-ray Crystal Structure of **1a.** Colorless crystal prisms of **1a** were grown by slow diffusion of diethyl ether into a THF solution of **1a** at -35 °C. Crystallographic data for **1a** were collected at the University of Washington X-ray crystallography laboratory (Table 3). A crystal of **1a** was mounted on a glass capillary with oil. All hydrogen atoms were located using a riding model. All non-hydrogen atoms were refined anisotropically by full-matrix least squares. The data was integrated and scaled using hkl-SCALEPACK.

Synthesis of $\text{fac}(\text{dppbz})\text{PtMe}_3(\text{N}(\text{Me})\text{SO}_2(p\text{-C}_6\text{H}_4(\text{CH}_2)_3\text{CH}_3))$ (9a**).** Compound **1a** (4 mg, 0.004 mmol) was weighed into an NMR tube equipped with a Teflon valve, and an excess of solid KH was added. A small stirbar was also added to the tube. THF was vacuum transferred and the suspension stirred for 2 days. The solution gradually

Table 3. X-ray Diffraction Data for **1a**

empirical formula	C ₄₇ H _{55.87} NO ₃ P ₂ PtS
fw	971.88
<i>T</i> (K)	130(2)
wavelength (Å)	0.710 73
cryst descriptn	colorless prism
space group	triclinic, <i>P</i> 1
unit cell dimens (Å, deg)	<i>a</i> = 10.8090(4) <i>b</i> = 14.5820(5) <i>c</i> = 14.6140(6) α = 100.0110(14) β = 101.9370(14) γ = 91.6000(15)
<i>V</i> (Å ³)	2214.41(14)
<i>Z</i> , ρ (mg/m ³)	2, 1.458
<i>M</i> (mm ⁻¹)	3.328
<i>F</i> (000)	985.7
cryst size (mm)	0.46 × 0.24 × 0.17
reflcn for indexing	689
θ range (deg)	2.15–28.32
index ranges	–12 ≤ <i>h</i> ≤ 14 –19 ≤ <i>k</i> ≤ 18 –18 ≤ <i>l</i> ≤ 19
reflcn collcd, unique completeness to θ (%)	16 628, 10 376 99.10
abs corr	semiempirical from equivalents
refinement method	full-matrix least squares on <i>F</i> ²
goodness of fit on <i>F</i> ²	<i>S</i> = 0.973
<i>R</i> ₁	0.0467
w <i>R</i> (<i>I</i> > 2 σ (<i>I</i>))	0.1147

turned pale yellow, and the formation of the deprotonated complex was monitored by ³¹P NMR (after removal of the magnetic stirbar) by the disappearance of the resonance for **1a** (18.1 ppm, *J*_{Pt–P} = 1028) and the appearance of a new resonance at 12.2 ppm with a Pt–P coupling of 1086 Hz. When the deprotonation was complete, excess MeI (~0.05 mL) was vacuum transferred into the tube. White KI precipitate formed immediately, and the solution turned colorless. The solution was filtered while cold, the THF was removed, and C₆D₆ was added for NMR analysis. ¹H NMR (C₆D₆): δ –0.004 (t w/Pt satellites, 3H, ³*J*_{P–H} = 8.0, ²*J*_{Pt–H} = 66, Pt–CH₃ trans to N), 0.86 (t, 3H, ³*J*_{H–H} = 7.0, –CH₂CH₂CH₂CH₃), 1.20 (m, 2H, –CH₂CH₂CH₂CH₃), 1.42 (m, 2H, –CH₂CH₂CH₂CH₃), 2.24 (vt w/Pt satellites, 6H, ³*J*_{P–H} = 6.6, ²*J*_{Pt–H} = 60, Pt–CH₃ cis to N), 2.38 (t, 2H, ³*J*_{H–H} = 7.6, –CH₂CH₂CH₂–CH₃), 2.73 (br s, 3H, PtN–CH₃), 6.8–8.2 (m, 24H, protons of phosphine and sulfonamide aryl rings, unresolved). ³¹P{¹H} NMR (C₆D₆): δ 21.6 (s w/Pt satellites, ¹*J*_{Pt–P} = 1032).

Synthesis of (dppbz)PtMe(NHSO₂(*p*-C₆H₄(CH₂)₃CH₃)) (4a). (dppbz)PtMe₂ (4 mg, 0.006 mmol) was weighed into an NMR tube equipped with a Teflon valve and dissolved in benzene. A 96 μ L volume of a 0.0621 M solution of trifluoromethanesulfonic acid in toluene (0.006 mmol) was added via syringe, and the mixture was allowed to react overnight. The solvent was removed in vacuo. The potassium salt of 4-*n*-butylbenzenesulfonamide was added (2 mg, 0.008 mol), and then C₆D₆ was vacuum transferred into the tube. The reaction was complete after 1 h, as observed by ³¹P{¹H} NMR. The solution was filtered into another NMR tube to remove potassium triflate, and the product was characterized by ¹H and ³¹P{¹H} NMR. ¹H NMR (C₆D₆): δ 0.82 (t, 2H, ³*J*_{H–H} = 7.3, –CH₂CH₂CH₂CH₃), 0.84 (dd w/Pt satellites, ³⁴ 3H, ²*J*_{Pt–H} = 55, Pt–CH₃), 1.16 (m, 2H, –CH₂CH₂CH₂–CH₃), 1.37 (m, 2H, –CH₂CH₂CH₂CH₃), 2.33 (t, 2H, ³*J*_{H–H} = 7.6, –CH₂–CH₂CH₂CH₃), 4.24 (br d, ³*J*_{P–H} = 2.6, Pt–NH), 6.8–8.0 (m, 24H, protons of phosphine and sulfonamide aryl rings, unresolved). ³¹P{¹H} NMR (C₆D₆): δ 50.3 (s w/Pt satellites, ¹*J*_{Pt–P} = 1865, P trans to CH₃), 41.2 (s w/Pt satellites, ¹*J*_{Pt–P} = 3625, P trans to NHSO₂R).

Synthesis of Sulfonamides. 3a. *N*-Methyl-4-*n*-butylbenzenesulfonamide was prepared by a modification of a literature procedure for the

preparation of *N*-methylbenzenesulfonamide.³⁵ *n*-Butylbenzenesulfonyl chloride (1.64 g, 7.04 mmol) was reacted with an excess of a 40% w/w solution of methylamine in water (3.2 mL, 35.7 mmol). The reaction mixture was heated on a steam bath for 15 min. The product was extracted three times with 15 mL portions of CH₂Cl₂. The organic fractions were combined, washed with water (3 × 5 mL) and then dried over MgSO₄. The solvent was removed in vacuo by rotary evaporation to yield the product as a clear oil. Yield: 1.45 g, 90%. ¹H NMR (C₆D₆): δ 0.81 (t, 3H, ³*J*_{H–H} = 7.3, –CH₂CH₂CH₂CH₃), 1.13 (m, 2H, –CH₂CH₂CH₂CH₃), 1.32 (m, 2H, –CH₂CH₂CH₂CH₃), 2.06 (d, 3H, N–CH₃), 2.28 (t, 2H, ³*J*_{H–H} = 7.7, –CH₂CH₂CH₂CH₃), 3.82 (s, 1H, NH), 6.86 (d, 2H, ³*J*_{H–H} = 8.0, aryl protons *ortho* to sulfonamide), 7.77 (d, 2H, ³*J*_{H–H} = 8.0, aryl protons *meta* to sulfonamide).

6a. 4-*n*-Butylbenzenesulfonamide (53.5 mg, 0.251 mmol) and 18-crown-6 (67 mg, 0.253 mmol) were dissolved in THF, and an excess of KH was added. The reaction mixture was stirred for 2 h and then filtered through glass wool and diatomaceous earth. The solvent was removed under vacuum, and the white crystalline product was recrystallized from THF/pentane. Yield: 97 mg, 75%. ¹H NMR (C₆D₆): δ 0.82 (t, 3H, ³*J*_{H–H} = 7.3, –CH₂CH₂CH₂CH₃), 1.20 (m, 2H, –CH₂CH₂CH₂–CH₃), 1.45 (m, 2H, –CH₂CH₂CH₂CH₃), 2.44 (t, 2H, ³*J*_{H–H} = 7.6, –CH₂–CH₂CH₂CH₃), 2.67 (s, 1H, NH), 3.35 (br s, 24H, crown ether protons), 7.03 (d, 2H, ³*J*_{H–H} = 8.0, aryl protons *ortho* to sulfonamide), 8.48 (d, 2H, ³*J*_{H–H} = 8.0, aryl protons *meta* to sulfonamide).

8a. *N,N*-Dimethyl-4-*n*-butylbenzenesulfonamide was prepared as follows: The potassium salt of **3a** (5 mg) was added to an NMR tube fitted with a Teflon valve. An excess of iodomethane (~0.2 mL) was added via vacuum transfer. The excess iodomethane was removed under vacuum following precipitation of KI, and C₆D₆ was added. ¹H NMR (C₆D₆): δ 0.81 (t, 3H, ³*J*_{H–H} = 7.3, –CH₂CH₂CH₂CH₃), 1.14 (m, 2H, –CH₂CH₂CH₂CH₃), 1.32 (m, 2H, –CH₂CH₂CH₂CH₃), 2.27 (s, 6H, N–CH₃), 2.28 (t, 2H, ³*J*_{H–H} = 7.7, –CH₂CH₂CH₂CH₃), 6.87 (d, 2H, ³*J*_{H–H} = 8.0, aryl protons *ortho* to sulfonamide), 7.67 (d, 2H, ³*J*_{H–H} = 8.0, aryl protons *meta* to sulfonamide).

10a. The sulfonamide dimer CH₂(N(Me)SO₂(*p*-C₆H₄(CH₂)₃CH₃))₂ was prepared by modification of a literature procedure for the analogous *p*-tolylsulfonamide dimer.²¹ HN(Me)SO₂(*p*-C₆H₄(CH₂)₃CH₃) (450 mg, 1.98 mmol) was dissolved in xylenes. A 0.140 mL volume of DMSO (1.97 mmol) was added, followed by 10 mg of solid P₂O₅. The reaction vessel was sealed with a Teflon stopcock and heated at 150 °C for 3 h. The solution was decanted into a separatory funnel and neutralized with a 10% NaOH solution. Upon addition of the base, the product precipitated from solution. The xylene fraction containing the precipitate was collected and the solvent removed under vacuum. The oily white residue was dried under vacuum overnight. ¹H NMR (C₆H₆): δ 0.81 (t, 6H, ³*J*_{H–H} = 7.3, –CH₂CH₂CH₂CH₃), 1.12 (m, 4H, –CH₂CH₂CH₂–CH₃), 1.31 (m, 4H, –CH₂CH₂CH₂CH₃), 2.27 (t, 4H, ³*J*_{H–H} = 7.7, –CH₂–CH₂CH₂CH₃), 2.75 (s, 6H, N–CH₃), 4.56 (s, 2H, –NCH₂N–), 6.82 (d, 4H, ³*J*_{H–H} = 8.3, aryl protons *ortho* to sulfonamide), 7.58 (d, 4H, ³*J*_{H–H} = 8.3, aryl protons *meta* to sulfonamide).

Sulfonamide Exchange Experiment. Compound **1b** (3.7 mg, 0.0043 mmol) and sulfonamide salt **6a** (2.4 mg, 0.0046 mmol) were weighed into an NMR tube equipped with a Teflon valve. C₆D₆ was added via vacuum transfer. The sample was heated at 85 °C in an oil bath for 3 days, quenching in an ice bath periodically for analysis by ¹H and ³¹P NMR. The amounts of Pt(IV) compounds **1b** and **1a** were monitored by ³¹P NMR (δ 18.0 ppm for **1b**, 17.9 ppm for **1a**), and the amounts of sulfonamide salts **6a** and **6b** were determined by ¹H NMR (aryl protons *meta* to sulfonamide; δ 8.34 ppm for **6b**, δ 8.38 for **6a**). Although the reaction was monitored for 3 days, equilibrium was reached after 25 h.

General Treatment of Kinetics Samples. A medium-walled NMR tube affixed to a 14/20 joint was loaded with 3 mg (0.003 mmol) of the Pt(IV)–sulfonamide complex **1** in the drybox. Triphenylmethane

(34) The ³*J*_{P–H} coupling constants could not be determined due to overlap of the Pt–Me resonance with the CH₃ resonance of the butyl chain.

(35) Banks, M. R.; Hudson, R. F. *J. Chem. Soc., Perkin Trans. 2* **1986**, 1211.

(0.8 mg, 0.003 mmol) was added as an internal standard. A small amount of benzene was added to the tube to dissolve the solids. The tube was attached to the vacuum line with a stopcock adapter, and the benzene was removed under vacuum. C₆D₆ was vacuum transferred into the tube (0.3–0.45 mL), the solution was kept frozen in liquid nitrogen, and the tube was flame-sealed under active vacuum.

A Neslab Exacal EX-250 HT elevated temperature bath was used to heat the NMR tubes at 100.0 °C. The thermolyses were quenched at various times for analysis by NMR by immersion of the tubes in cold water or ice water, and the tubes were stored in a freezer at –23 °C when not being heated. ¹H and ³¹P{¹H} NMR spectra were recorded on a Bruker DRX 499 spectrometer, using a delay time of 50 s. The reaction progress was monitored by integration of the signals of both the axial and equatorial methyl groups of the starting compound relative to the internal standard, averaging the integrals of three separate

acquisitions. The thermolyses were followed for 3 half-lives, and mass balance was confirmed after heating the reactions to completion.

Acknowledgment. This work was supported by the National Science Foundation (CHE-0137394) with initial funding from the Petroleum Research Fund, administered by the American Chemical Society. The X-ray structure determination was performed by Dr. W. Kaminsky at the University of Washington. We thank Brietta J. Smith for synthetic contributions.

Supporting Information Available: A CIF file for *fac*-(dppbz)PtMe₃(NHSO₂(*p*-C₆H₄(CH₂)₃CH₃)) (**1a**). This information is available free of charge via the Internet at <http://pubs.acs.org>. JA069191H